Neurobiology of Aging 78 (2019) 74–86

Contents lists available at ScienceDirect

Neurobiology of Aging

journal homepage: www.elsevier.com/locate/neuaging

Delayed daily activity and reduced NREM slow-wave power in the APPswe/PS1dE9 mouse model of Alzheimer's disease

Brianne A. Kent [a,1], Mateusz Michalik [b,1], Elliott G. Marchant [c], Kiana W. Yau [a], Howard H. Feldman [d], Ralph E. Mistlberger [b,**], Haakon B. Nygaard [a,*]

[a] Djavad Mowafaghian Centre for Brain Health, Department of Medicine, Division of Neurology, University of British Columbia, Vancouver, Canada
[b] Department of Psychology, Simon Fraser University, Burnaby, Canada
[c] Department of Psychology, Vancouver Island University, Nanaimo, Canada
[d] Department of Neurosciences, University of California, San Diego, USA

ARTICLE INFO

Article history:
Received 11 September 2018
Received in revised form 14 December 2018
Accepted 13 January 2019
Available online 14 February 2019

Keywords:
Alzheimer's disease
Circadian rhythms
Sleep
Transgenic model
EEG
Power spectra

ABSTRACT

Alzheimer's disease (AD) is associated with disrupted circadian rhythms and sleep, which are thought to reflect an impairment of internal circadian timekeeping that contribute to clinical symptoms and disease progression. To evaluate these hypotheses, a suitable preclinical model of AD is needed. We performed a comprehensive assessment of circadian rhythms and sleep in the $APP_{swe}/PS1_{dE9}$ (APP/PS1) mouse model using long-term in vivo electroencephalogram (EEG) monitoring and behavioral assays from 5 to 22 months of age. APP/PS1 mice were crossed with a PERIOD2::LUCIFERASE (PER2::LUC) mouse model to evaluate synchrony among peripheral circadian oscillators. The APP/PS1 mice exhibited a mild but persistent phase delay of nocturnal activity onset in 12:12h light:dark conditions, as well as a shift toward higher frequencies in the EEG power spectra compared to littermate controls. Our results suggest that APP/PS1 mice may not be the optimal preclinical model for studying the specific circadian changes associated with AD but that quantitative EEG may offer a sensitive measure of AD-associated changes in sleep quality that can be modeled in APP/PS1 mice.

1. Introduction

Alzheimer's disease (AD) is a progressive neurodegenerative disorder and the most common cause of dementia (Nygaard, 2013). The pathological drivers of AD are thought to include a gradual buildup of soluble brain amyloid-beta (Aβ), neuritic plaques, and tau-containing neurofibrillary tangles, emerging up to decades before clinical symptoms (Gordon et al., 2018). It is well documented that AD is also associated with disrupted circadian rhythms and sleep beginning during the preclinical stage of the disease (Ju et al., 2014; Musiek et al., 2018; Tranah et al., 2011; Yaffe et al., 2015). In a sample of 204 community-dwelling individuals with AD, 134 (65%) met diagnostic criteria for 1 or more of 5 major sleep disorders, and the rates were similar for those diagnosed with mild cognitive impairment (Guarnieri et al., 2012). The most common sleep disturbances among individuals with AD include nocturnal sleep fragmentation, increased daytime napping, decreases in specific stages of sleep including nonrapid eye movement (NREM) slow-wave sleep ([SWS], stage N3), and rapid eye movement sleep (REM), and loss of differentiation between NREM stages N1 and N2 (reviewed by (Mander et al., 2016) and (Cedernaes et al., 2017)). Sleeping difficulties are highly disruptive and have been cited as a leading cause of patients requiring institutional care (Bianchetti et al., 1995). Importantly, recent discoveries provide preclinical evidence that sleep (SWS in particular) directly impacts the pathophysiology of AD, by regulating production and clearance of Aβ (Ju et al., 2014, 2017; Lucey et al., 2018; Xie et al., 2013).

The timing of the sleep-wake cycle is regulated by a master circadian (~24h) pacemaker in the hypothalamic suprachiasmatic nucleus (SCN). The SCN pacemaker is entrained to daily light:dark (LD) cycles by direct input from the retina. SCN outputs coordinate the phase of circadian oscillators located elsewhere in the brain and in most peripheral organs and tissues, aligning behavioral and physiological rhythms with the solar day (Reppert and Weaver, 2002). Similar to the AD-associated changes in sleep, AD is associated with changes in circadian rhythms beginning early in the

* Corresponding author at: Djavad Mowafaghian Centre for Brain Health, University of British Columbia, 2215 Wesbrook Mall, Vancouver, BC V6T 1Z3. Tel.: +1 604 827 0600; Fax: +1 604 822 0361.
** Corresponding author at: Department of Psychology, Simon Fraser University, Burnaby, BC V5A 1S6. Tel.: +1 778 782 3462; Fax: +1 778 782 3427.
E-mail addresses: mistlber@sfu.ca (R.E. Mistlberger), haakon.nygaard@ubc.ca (H.B. Nygaard).
[1] Authors contributed equally to this work.

0197-4580/$ – see front matter © 2019 Elsevier Inc. All rights reserved.
https://doi.org/10.1016/j.neurobiolaging.2019.01.010

preclinical stage of disease, before symptom onset and cognitive impairment (Musiek et al., 2018). Individuals diagnosed with AD exhibit delayed (i.e., peaks later in the day) and lower amplitude daily rhythms in activity and core body temperature, compared to age-matched healthy controls (Satlin et al., 1995; Volicer et al., 2001). Importantly, the phase delay associated with AD (Satlin et al., 1995; Volicer et al., 2001) may differentiate individuals with AD from healthy aging, which is typically associated with phase advanced sleep-wake cycles (i.e., peak earlier in the day), as well as other types of dementia including frontotemporal lobar degeneration (Harper et al., 2001, 2005). Because sleep propensity and structure vary with circadian phase (Dijk and Czeisler, 1995), a delayed phase of sleep onset may therefore contribute to sleep disturbances experienced by patients with AD. For example, individuals diagnosed with delayed sleep phase syndrome exhibit different sleep structures and only half the amount of SWS compared to healthy volunteers when assessed with 2 nights of polysomnography (Watanabe et al., 2003). Thus, the phase delay in circadian timing may contribute to the reduced SWS also associated with AD.

Because changes in circadian rhythms and sleep occur early in disease, it is hypothesized that these changes may also contribute to cognitive decline and disease progression, and modulating circadian rhythms and sleep through noninvasive or pharmacological interventions may benefit a subset of patients with AD. To evaluate these hypotheses and test interventions, a suitable preclinical rodent model of AD is needed. Sleep and circadian rhythms have been assessed in several AD mouse models, including APP_{SWE}, $APP_{SWE}/PS1_{A246E}$, $APP_{SWE}/PS1_{P264L}$, $APP_{SWE}/PS1_{dE9}$, 3xTgAD ($APP_{SWE}/PS1_{M146V}/MAPT_{P301L}$), and 5xFAD ($APP_{SWE,FLO,LON}/PS1_{M146L,L286V}$) (Bano Otalora et al., 2012; Duncan et al., 2012; Jyoti et al., 2010; Kent et al., 2018; Knight et al., 2013; Roh et al., 2012; Sethi et al., 2015; Sterniczuk et al., 2010; Vloeberghs et al., 2004). Overall the results suggest that sleep and circadian rhythms are affected in AD models; however, results vary between studies, likely in part due to differences in transgenes, background strain of the lines, or variation in experimental protocols. To our knowledge, no model has been shown to exhibit both the delayed phase of entrainment and reduced SWS characteristic of human AD. Furthermore, alignment between the SCN and peripheral clocks located elsewhere in the brain, organs, and tissues has not been evaluated in a mouse model of AD. Although it is largely assumed that disrupted circadian rhythms in AD are caused by the dampening of the SCN, there is evidence that AD pathology may be disrupting synchrony among circadian oscillators (Cermakian et al., 2011; Chauhan et al., 2017; Chen et al., 2014; Kent, 2014; Wu et al., 2006). Internal circadian misalignment, as opposed to misalignment of the SCN with external daylight, would cause similar behavioral symptoms but require different interventions (Chauhan et al., 2017; Kent, 2014).

Here, we conducted a detailed assessment of both sleep and circadian rhythm dynamics in the $APP_{SWE}/PS1_{dE9}$ (APP/PS1) transgenic AD mouse model, a widely used murine model in preclinical AD research. Studies examining sleep and circadian rhythmicity in this model are limited but suggest that changes in sleep develop between 6 and 9 months of age (Bano Otalora et al., 2012; Roh et al., 2012). To investigate these changes in more detail and with careful assessment of circadian rhythmicity, mice were examined from 5 to 22 months of age using a variety of behavioral assays, in vivo electroencephalogram (EEG) recordings, and histology. Behavioral assays included an assessment of LD-entrained circadian rhythms, the circadian period in constant dark, the circadian waveform in LD, and the phase shift and masking responses to light in TG and WT mice. The timing of the master clock relative to several peripheral clocks was assessed by crossing the APP/PS1 mice with a PERIOD2::LUCIFERASE (PER2::LUC) mouse model, to create a clock gene-driven bioluminescence assay (Yoo et al., 2004). Peripheral circadian dynamics were further probed using a restricted feeding paradigm to assess food-anticipatory activity, which is a circadian clock-controlled process that is independent of the SCN (Mistlberger, 2009).

2. Materials and methods

2.1. Subjects

We assessed circadian rhythms and sleep in the APP/PS1 mouse model of AD (APPswe/PSEN1dE9) (Jankowsky et al., 2004). The mice were a gift from Dr. Cheryl Wellington at the University of British Columbia. The APP/PS1 mice (The Jackson Laboratory) coexpress 2 transgenes from the murine prion promoter: a chimeric mouse/human APP650 cDNA containing the Swedish (K670 M/N671 L) mutations and the human PS1 gene with a deletion of exon 9. APP/PS1 mice were maintained on a hybrid C3H/H3J × C57B6 background.

A total of 86 male and female mice were used in the following experiments: 42 (females = 32) for circadian behavioral recordings, 17 (females = 17) for in vivo EEG recordings, and 27 (females = 12) for histological analysis. These were distinct cohorts. The behavioral recordings were conducted longitudinally using the same 42 mice for all behavioral manipulations, which were split into 2 cohorts (tested sequentially, 3 months apart). These cohorts were combined for analyses whenever possible. The variability was a result of the inherent time constraints of a longitudinal study (i.e., limited to testing 1 manipulation at a time), prioritizing the circadian parameters that were most interesting, and naturally occurring attrition as the mice aged. All the analyses were conducted within time points, which compare TG to WT littermates, balanced with regard to sex. The first cohort was only female because that is what had been used in Roh et al., 2012, which reported sleep disturbances in this model. The second cohort had equal numbers of males and females for each genotype. The intention was to identify phenotypes of interest in the females and then follow-up in both males and females, but given the subtle phenotypes identified, this study was not powered to study sex-specific effects. Supplementary Table 1 gives the exact breakdown of sex per analysis.

APP/PS1 mice were crossed with the PERIOD2::LUCIFERASE (PER2::LUC) mouse line (The Jackson Laboratory, 006852, $mPer2^{Luc}$) (Yoo et al., 2004). The PER2::LUC were on a C57B6 background. We first crossed male APP/PS1 mice with female $Per2^{Luc/Luc}$ mice and then the male offspring heterozygous for both the APP/PS1 and $Per2^{Luc}$ were crossed with $Per2^{Luc/Luc}$ females. We used both APP/PS1xPer2$^{Luc/+}$ (heterozygous $Per2^{Luc}$) and APP/PS1xPer2$^{Luc/Luc}$ (homozygous $Per2^{Luc}$) mice in experiments. A total of 25 (females = 11) were used at 6 months of age, and 14 (females = 0) were used at 12 months of age. The APP/PS1xPer2$^{Luc/+}$ and APP/PS1xPer2$^{Luc/Luc}$ were heterozygous for APP/PS1.

All procedures involving experimental animals were approved by the Canadian Council of Animal Care, the University of British Columbia Committee on Animal Care, and the Simon Fraser University Animal Care Committee (permit 1106p-09).

2.2. Genotyping

DNA was extracted from mouse ear notches using the RedExtract-N-Amp Tissue PCR kit (Sigma, Catalog # XNAT).

2.3. Circadian behavioral recordings

Mice were housed in standard mouse cages with bedding materials and a translucent orange igloo. Cages were contained within

isolated cabinets, and locomotion was recorded using infrared motion sensors monitored with Clocklab (Actimetrics). Lighting was provided via LED lights placed on surrounding cabinet walls above the cage with an average illuminance of 7 lux. Mice were given access to food and water *ad libitum*, unless specified otherwise. Cages were changed every 2 weeks during the dark phase to minimize disturbances, except during restricted feeding experiments when they were changed after food was removed. Representative actograms from the various experiments are presented in Supplementary Fig. S1.

2.4. EEG implantation

Mice were deeply anesthetized with isoflurane throughout the procedure. A midline incision was made, and 4 burr holes were manually drilled through the skull at the following coordinates relative to bregma: AP: +2 mm, ML: +/− 1.5 mm and AP −4 mm, ML +/− 1.5 mm. Four stainless steel screw electrodes were inserted through holes of a prefabricated EEG headmount (catalog number 8406-SL; Pinnacle Technology) and manually rotated into the predrilled burr holes. The headmount was secured with a layer of dental cement (catalog number 525000; A-M Systems, Sequim, WA, USA). Two EMG electrode wires were inserted under the nuchal muscles. Meloxicam (5 mg/kg, IP), buprenorphine (0.07 mg/kg, SC), and lidocaine (7 mg/kg, SC along incision site) were used for analgesia during surgery, and meloxicam and buprenorphine were administered for 3 days postop. Lactated ringer (10 mL/kg) was provided at the end of surgery and during postop if dehydration was a concern. All mice were allowed to recover for at least 7 days before EEG recordings.

2.5. EEG recordings

Mice were transferred to EEG recording cages, attached to recording cables, and habituated for 2 days before recording EEG for analysis. Mice were recorded using an in vivo EEG monitoring system (8200-K1-SE3, 8236; Pinnacle Systems). Each mouse underwent 72 hours of continuous EEG recording in a circular clear, plexiglass recording cage and was maintained on a regular 12:12 LD cycle with full access to food and water.

2.6. Circadian analysis

Circadian rhythm measures included phase of entrainment to the 12:12 LD cycle, mean and peak activity levels, masking and phase shifting responses to light, endogenous period in DD and LL, rhythm amplitude change from LD to LL lighting conditions, and rate of entrainment to shifted LD and scheduled mealtime. Circadian analysis was conducted using Clocklab (Actimetrics) and GraphPad Prism 7.0a (GraphPad Software Inc, La Jolla, CA, USA). Onsets of nocturnal activity or premeal activity were determined by experimenters blinded to genotype using Clocklab (Actimetrics) to view data.

Relative amplitudes were calculated using Clocklab (Actimetrics), taking into consideration the 10 most active and 10 least active hours on average for each mouse using the same 3-week periods used in nocturnal activity onset determination. Relative amplitude was calculated using the formula:

$$\textit{Relative Amplitude } (RA) = \frac{M_{10}\,Avg - L_{10}\,Avg}{M_{10}\,Avg + L_{10}\,Avg}$$

Where M_{10} *Avg* is the average activity in the most active 10 hours, and L_{10} *Avg* is the average activity in the least active 10 hours.

2.7. Sleep analysis

Sleep stage and wake analysis and power spectra analysis were completed on the final 24 hours of the EEG recordings. An investigator, blinded to genotype, scored the 24 hours EEG traces manually for wake and sleep using a 10-second epoch duration and Sirenia Sleep Pro software (Pinnacle Technology). The data were first analyzed using cluster scoring, evaluating power by specific frequency bands (e.g., delta, theta, alpha, beta, and gamma) for the EEG and EMG channels, to identify bouts of sleep, wake, and transition periods. The scoring of each 10-second epoch was then confirmed through visual inspection by evaluating the recording and corresponding spectral plot. Wake was defined by low-amplitude EEG, dominant EEG frequency >4 Hz, and high-amplitude EMG. NREM sleep was defined by high-amplitude EEG, dominant EEG frequency <4 Hz, and low-amplitude EMG. REM was defined by a dominant frequency between 4 and 8 Hz in the EEG recording, uniform EEG waveforms, low-amplitude EMG, and occurring at a transition from NREM to wake. An epoch was defined according to which state was >50% of the 10- second epoch. The EEG recordings were rated for clarity, and 5 mice were removed from the analysis because of poor quality EEG signal or excessive artifact. Percentage of time spent in each sleep or wake state was calculated by dividing by total time (24 hours). Individual epochs containing artifact were not included in the power spectra analysis but were included in the estimates of time spent in each state (i.e., each epoch that included artifact was scored as wake, NREM, or REM). Percentage of time spent in wake, NREM, and REM stages for the TG and WT were compared using a 2-tailed unpaired *t*-test. Statistical significance was set at $p \leq 0.05$. Power spectral analysis was completed by using Fast Fourier Transform to decompose the EEG time series into a voltage by frequency spectral graph, with power being the square of the EEG magnitude, and magnitude being the integral average of the amplitude of the EEG signal. Power data were evaluated raw and also normalized as a percentage of the accumulated power from 0.1 to 50 Hz. Statistical analyses were performed using GraphPad Prism 7.0a (GraphPad Software Inc, La Jolla, CA, USA). Statistical significance was determined by 2-way analysis of variance (ANOVA) and followed by post hoc *t*-tests using the Bonferroni correction to compare specific frequency bands when a significant interaction was observed. All data are expressed as mean ± standard error of the mean (SEM).

2.8. Peripheral oscillator analysis

APP/PS1xPER2::LUC mice were sacrificed by rapid decapitation between ZT 9 and 12, and the brains were rapidly extracted and immediately chilled in 4C Hanks' Balanced Salt Solution (HBSS). Three hundred micro metre sections containing SCN were obtained using a vibratome, and SCN was dissected out using a scalpel under a dissection microscope. Samples of the liver, lung, stomach, and spleen were dissected out concurrently with brain extraction and vibratome sectioning. Dissected SCN were placed in 35 mm petri dishes with 1 mL modified DMEM solution with beetle luciferin (Yamazaki and Takahashi, 2005) on top of a Millipore cell culture insert (PICMORG50). Peripheral tissues were maintained in the same media without inserts. Luminescence was measured at 10 minute intervals using a LumiCycle 32 channel luminometer (Actimetrics). Circular statistics were analyzed using the circular package (v0.4–93) for R (v3.2.3).

See the Supplementary Section for additional methods detailing immunohistochemistry.

3. Results

3.1. APP/PS1 mice exhibit cortical Aβ deposits at 7 months of age

The APP/PS1 mouse model used here has been shown to develop Aβ deposits at about 6 months of age, with levels accumulating by 9 months of age (Roh et al., 2012). We confirmed a similar accumulation in our mouse line, with Aβ staining increasing significantly from 7 to 10 months of age in TG ($p = 0.0006$; Fig. S2). We also chose these time points for histology because the onset of sleep abnormalities in this mouse model has been reported to occur between 6 and 9 months of age (Roh et al., 2012).

3.2. APP/PS1 mice exhibit a small but persistent delayed phase of entrainment to LD

A feature of AD in humans is a delayed phase of entrainment, marked by peaks of activity and core body temperature occurring later in the day compared to healthy aging (Harper et al., 2001, 2005; Satlin et al., 1995; Volicer et al., 2001). To examine the phase of entrainment of activity rhythms, the timing of nocturnal activity onset in WT and TG mice was quantified for at least 3 weeks at 4 age ranges (5–6, 9, 12, and 19 months of age). Onset of nocturnal activity is shown in Fig. 1. Ages chosen represent advancing stages of Aβ accumulation. Activity onsets during the 3-week windows were averaged for each mouse before grouped analysis. By 5–6 months, activity onset was delayed in TG mice ($p < 0.01$, Fig. 1A and E). The delay persisted at 9 months ($p < 0.01$, Fig. 1B and F) and 19 months ($p < 0.05$, Fig. 1D and H) of age. The phase delay did not attain statistical significance at 12 months of age ($p = 0.053$, Fig. 1C and G), likely because fewer mice were available for analysis at this time point, due to the various lighting manipulations that were carried out. Of note, at 3–4 months of age, a subtle delay of activity onset was observed in female, but not in male, TG mice compared to WT mice, suggesting that the phenotype progression may differ by sex and represents an area of potential interest for follow-up studies (Fig. S3).

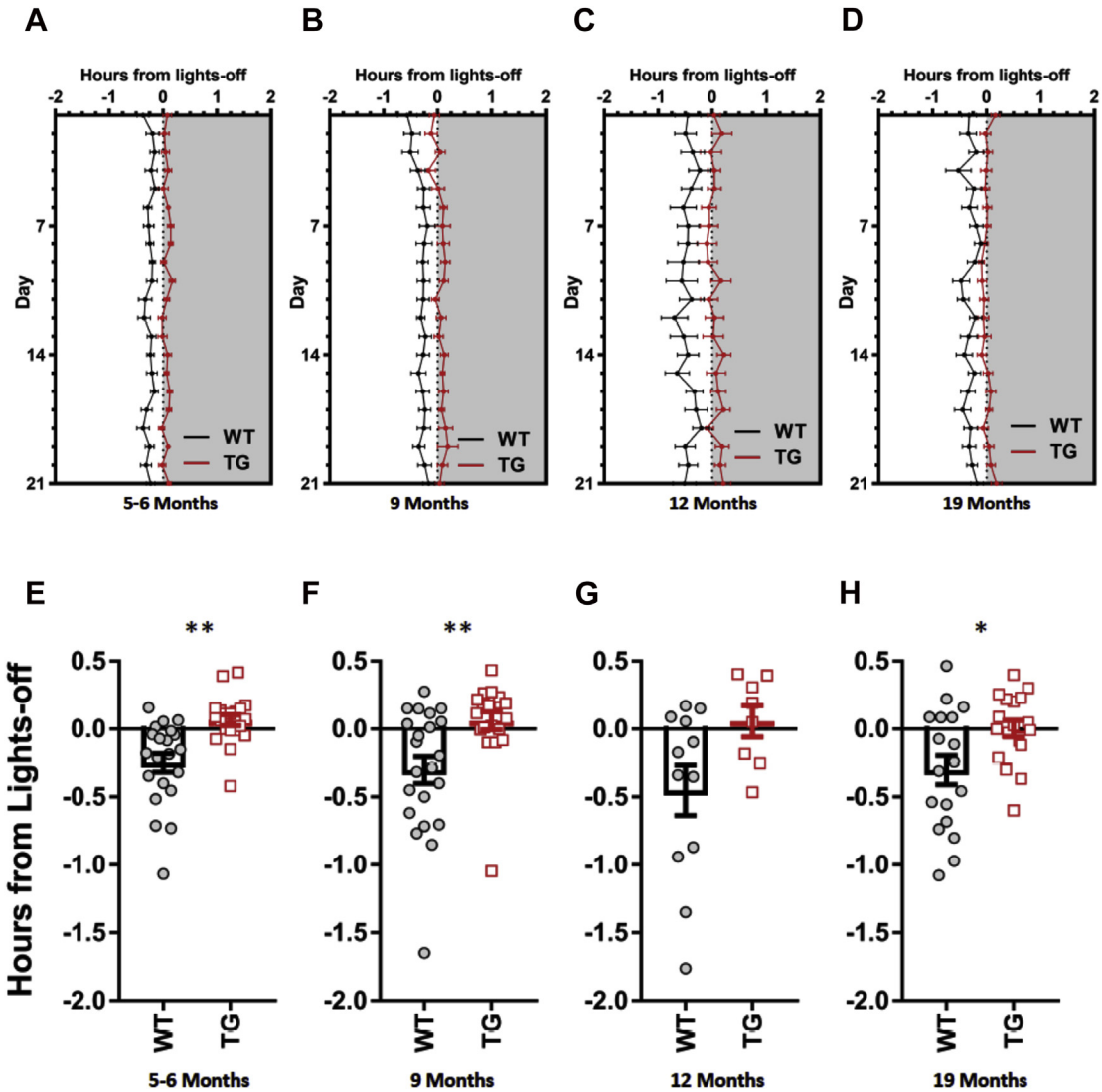

Fig. 1. Nocturnal activity onset in LD conditions for 21 days at 5–6 months (A), 9 months (B), 12 months (C), and 19 months (D). Group mean and individual mouse data at 5–6 months (E), 9 months (F), 12 months (G), and 19 months (H), corresponding to the same periods used in A–D. WT data are presented in black and TG data are presented in red. Data are expressed as the mean ± SEM. $^{*}p < 0.05$, $^{**}p < 0.01$, independent *t*-test. (For interpretation of the references to color in this figure legend, the reader is referred to the Web version of this article.)

3.3. The delayed phase of entrainment in APP/PSI mice is not caused by differences in pacemaker period (τ) or phase shift response to light

A delayed phase of entrainment can be explained by a lengthening of the endogenous period (τ) of the circadian pacemaker (Pittendrigh and Daan, 1976). To measure τ, TG and WT mice were held under DD conditions or LL conditions for 10 days. Fig. 2A–D shows the τ estimates obtained using χ^2 periodogram. Independent *t*-tests revealed no statistically significant differences between genotype at any age ($p > 0.05$).

Circadian rhythms entrain to daily LD cycles because the phase of the SCN master pacemaker can be shifted by exposure to light at pacemaker phases when environmental light is normally minimal or absent (Pittendrigh and Daan, 1976). A delayed phase of entrainment to LD cycles could thus occur if the pacemaker responsivity to light at night is altered. Responsivity can be assessed by measuring the size of phase shifts to a single brief exposure to

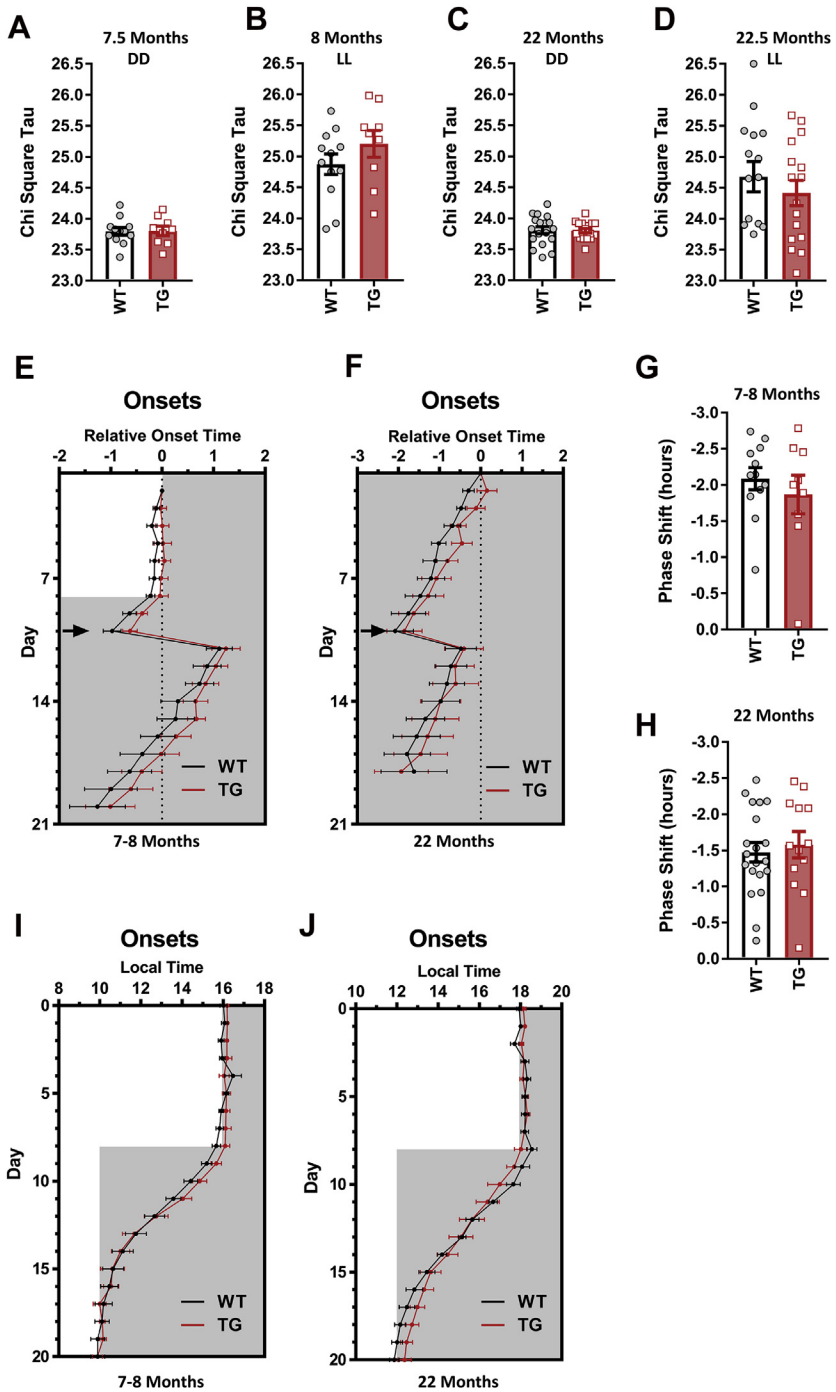

Fig. 2. Periodicity estimates at 7.5 months under DD conditions (A), at 8 months under LL conditions (B), at 22 months under DD conditions (C), and at 22.5 months under LL conditions (D). The endogenous τ (period) estimates were quantified using χ^2. Phase shifts and activity onsets at 7–8 months of age (E, G) and 22 months of age (F, H) following a 15-minute light pulse 3 hours after activity onset. Activity onset at 7–8 months of age (I) and 22 months of age (J) before and after a 6-hour phase advance in the LD schedule. Shaded gray regions correspond to lights-off (E, F, I, J). TG data are shown in red and the WT data are shown in black. Data are expressed as the mean ± SEM. (For interpretation of the references to color in this figure legend, the reader is referred to the Web version of this article.)

light in mice free-running in DD. TG and WT mice were therefore maintained in DD for at least 48 hours and then exposed to a 15-minute light pulse 3 hours after the previous dark phase onset. Light induced phase shifts were assessed at 7–8 months and 22 months of age (Fig. 2E–H). Phase shifts were quantified by fitting a regression line to activity onsets on the 7 days following the day of the light pulse and comparing the difference between the activity onset on the day of the light pulse and the projected activity onset on the following day. Independent *t*-tests revealed no statistically significant differences between genotype at any age ($p > 0.05$; Fig. 2G and H).

Another way to assess pacemaker responsivity to light is to shift the LD cycle to which mice are entrained and measure the rate of re-entrainment. To examine rate of re-entrainment, the LD cycle was advanced 6 hours, Fig. 2I and J shows the onset of nocturnal activity at 7–8 months and 21 months of age. Activity onsets were determined by experimenters blind to genotype using Clocklab data analysis software to display actograms. Independent *t*-tests revealed no differences between genotypes in the time of activity onset on any day after the 6 hours LD advance, or in the number of days required for onsets to realign with lights off (all $p > 0.05$).

3.4. The delayed phase of entrainment in APP/PSI mice is not associated with the level and/or timing of activity at night

Although environmental light is the primary stimulus by which circadian rhythms entrain to local time, some nonphotic stimuli, including spontaneous or stimulated locomotor activity (exercise), can shift circadian phase, modulate τ in DD, or alter the phase of entrainment to LD (Webb et al., 2014). These studies indicate that in mice, spontaneous locomotor activity early in the night tends to phase advance the circadian pacemaker, whereas activity later in the night delays the pacemaker. It is therefore possible that the delayed phase of LD entrainment in TG mice is caused by changes in the intensity or timing of nocturnal locomotion. There was no statistically significant difference in total daily activity at any time point (Fig. 3A–D). Interdaily stability (IS), a measure of day-to-day variability in the phase relationship between the rest-activity rhythm and the external LD cycle (Witting et al., 1990), was also calculated for each mouse to explore whether the phase difference between genotypes was due to stability of entrainment. At all 4 time points, there was no significant difference in IS (all $p > 0.05$).

Nocturnality was assessed (Fig. 3E–H) following visual inspection of the group activity waveforms, which suggested that the TG mice, compared to WT mice, may express a greater proportion of nocturnal activity during the second half of the night (Fig. 3I–L). Nocturnality ratio was quantified by calculating the ratio of activity in the first 6 hours of the night to activity in the second 6 hours of the night, at 5–6 months (Fig. 3E), 9 months (Fig. 3F), 12 months (Fig. 3G), and 19 months (Fig. 3H) of age. Independent *t*-tests revealed that there was no statistically significant difference in the distribution of nocturnal activity between genotypes at the 5–6 month and 12-month time points (all $p > 0.05$). There was a statistically significant difference in the nocturnal distribution of activity detected at 9 months ($p < 0.05$) and 19 months of age ($p < 0.001$), with TG mice being more active in the latter 6 hours of the dark phase compared to WT mice (Fig. 3F and H).

3.5. The delayed phase of entrainment in APP/PS1 mice is not caused by differences in acute ("masking") effects of light on activity

Nocturnal activity onset in WT mice anticipated lights-off by 15 minutes on average, whereas TG mice on average did not become active until after lights off (Fig. 1). In nocturnal rodents, light suppresses activity ("negative masking") and dark stimulates activity ("positive masking"). It is therefore possible that the delay of activity onset in the TG mice reflects an enhanced negative masking effect of light. To test this hypothesis, mice at 7 months of age were exposed to a 2:2 LD cycle (lights on for 2 hours, then off for 2 hours) for 24 hours (Fig. 3M–N). Light exposure at night markedly suppressed activity in the TG and WT mice, and there were no significant differences between genotype in any 2 hour block at 7 months of age (Fig. 3O, all $p > 0.05$).

3.6. Delayed phase of entrainment in APP/PS1 mice is not caused by loss of retinal melanopsin

Melanopsin-expressing retinal ganglion cells are intrinsically photoreceptive, project to the SCN pacemaker, and are required for pacemaker responses to light (La Morgia et al., 2017; Reppert and Weaver, 2002). There is 1 report of reduced melanopsin expression in postmortem analysis of retinas from patients with AD (La Morgia et al., 2016), and 1 report of reduced expression in APP/PSI mice (Perez et al., 2009). Immunocytochemical staining of retinas from mice used in the present study yielded no evidence for a reduction in melanopsin expression in TG mice compared to WT mice at 7 months or 10 months of age ($p > 0.05$, Fig. S4). These time points were chosen for histology because sleep abnormalities in this mouse model were previously reported to occur between 6 and 9 months of age (Roh et al., 2012).

3.7. The delayed phase of entrainment in APP/PS1 mice is not associated with a change in amplitude of activity rhythms under LD conditions

Another prominent feature of circadian rhythms in humans with AD is fragmentation and reduced amplitude of the rest-activity rhythm (e.g., more sleep/rest in the day and more wake/activity at night). To quantify amplitude of daily activity rhythms measured by the infrared motion sensors, we used the 3-week blocks of activity data at each of the 4 time points used above in nocturnal activity onset determination. Relative amplitude estimates are presented in Supplementary Fig. S5. There was a statistically significant difference in amplitude between TG and WT at 5–6 months (Fig. S5A) but not at 9 months (Fig. S5B), 12 months (Fig. S5C), or 19 months (Fig. S5D) of age ($p > 0.05$).

3.8. Measures of behavioral state fragmentation are not altered in APP/PS1 mice

Activity in mice is not continuous throughout the night but occurs in bouts alternating with brief periods of rest. Bouts also occur during the day. Procedures that reduce circadian amplitude (e.g., long-term exposure to constant light) or eliminate circadian rhythms (e.g., SCN ablation) typically increase the daily number and decrease the duration of activity bouts. This may also be associated with an increase in the power of ultradian (<24 hours) rhythmic components in rest-activity data, particularly at harmonics of the circadian period. To quantify bout number and duration, the Clocklab algorithm was applied to the 3-week blocks of data at 5–6 months, 9 months, 12 months, and 19 months of age (Fig. S6). There were no statistically significant differences between TG and WT in activity bout number or duration ($p > 0.05$). Results of Clocklab analysis are summarized in Supplementary Fig. S6.

To quantify ultradian rhythmicity, the Lomb Scargle periodogram was applied to the 3-week blocks of activity data at each of the 4 time points (5–6 months, 9 months, 12 months, and 19 months of age; Fig. S7). There were no statistically significant differences

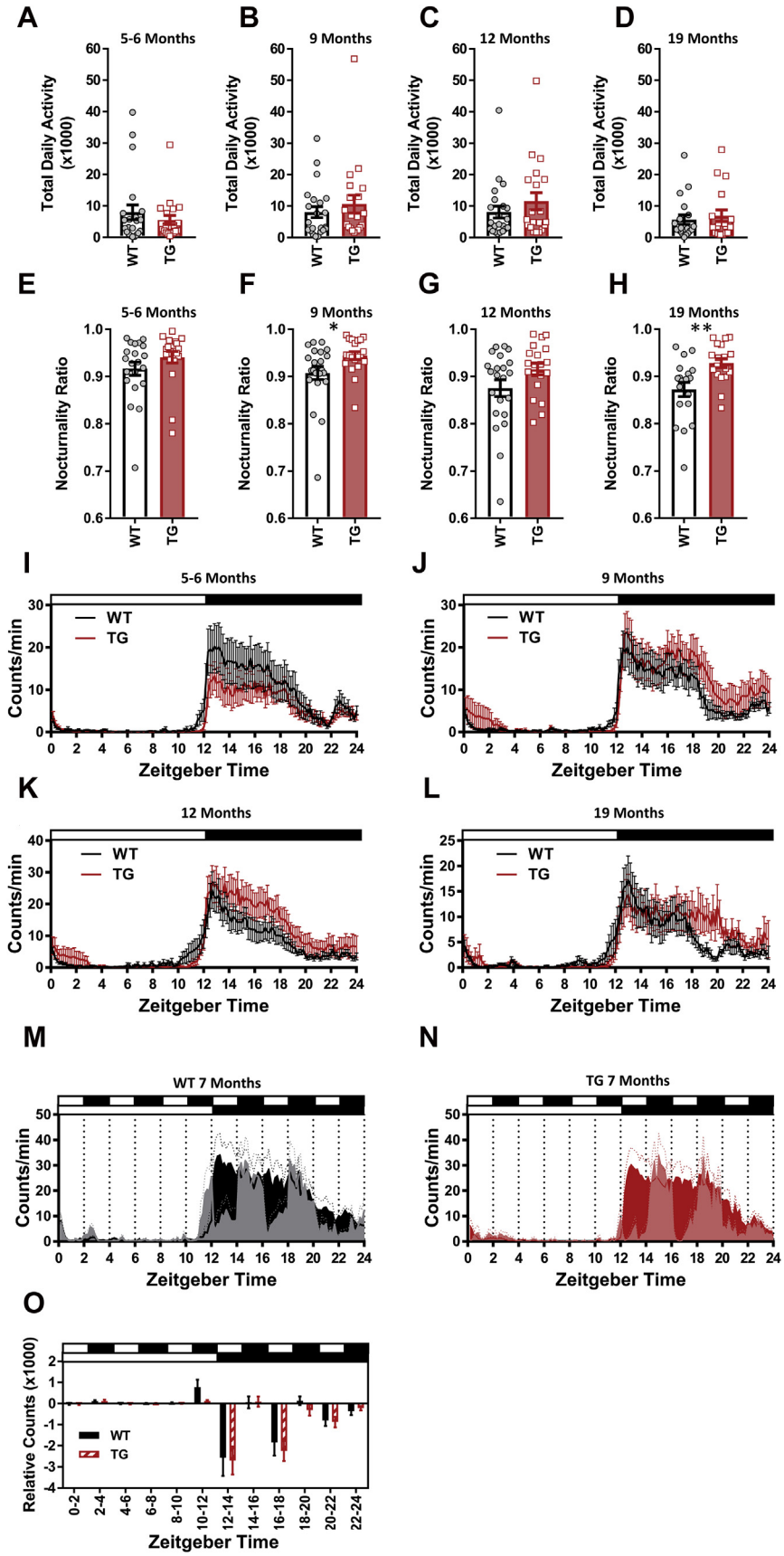

Fig. 3. Total daily activity in APP/PS1 mice at 5–6 months (A), 9 months (B), 12 months (C), and 19 months (D) of age. Nocturnality in APP/PS1 mice at 5–6 months (E), 9 months (F), 12 months (G), and 19 months (H) of age. Raw activity across 24 hours under LD conditions for 21 days at 5–6 months (I), 9 months (J), 12 months (K), and 19 months (L) of age. Masking test (2:2 LD) at 7 months of age (M–O). Raw activity counts under 12:12 LD conditions and 2:2 masking conditions for WT (M) and TG (N). Normalized activity counts comparing WT and TG activity under 12:12 and 2:2 LD conditions (O). TG data are shown in red and the WT data are shown in black. Data are expressed as the mean ± SEM. $^{*}p < 0.05$, $^{**}p < 0.01$, independent *t*-test. (For interpretation of the references to color in this figure legend, the reader is referred to the Web version of this article.)

between TG and WT in ultradian rhythmicity. The results are summarized in Supplementary Fig. S7.

The same 3-week blocks were also used to calculate intradaily variability (IV), a measure of behavioral fragmentation. No significant differences in IV were detected at any of the 4 time points studied (all $p > 0.05$, data not shown).

3.9. Synchrony among peripheral oscillators is not impaired in APP/PS1xPER2::LUC mice at 6 and 12 months of age

SCN pacemaker outputs coordinate the timing of circadian oscillators embedded in most peripheral organs and tissues. Local oscillators in turn drive daily rhythms of organ functions and outputs (e.g., metabolic hormones and neural autonomic signals), some of which may directly or indirectly affect SCN timing. Therefore, it is possible that changes in the phase or amplitude of circadian rhythms in patients with AD are due to changes in the timing of peripheral oscillators relative to the SCN pacemaker. To investigate whether the circadian behavioral phenotype in APP/PS1 mice was associated with changes in alignment between the SCN pacemaker and peripheral clocks, we created a novel mouse line by crossing the APP/PS1 and PER2::LUC mouse models. By measuring timing of PER2::LUC bioluminescence in explanted SCN, lung, spleen, stomach, and liver, we were able to assess potential effects of the APP/PS1 transgenes on internal circadian synchrony. The phase of oscillations was determined by the timing of the first peak after 24 hours in culture. Fig. 4 shows the peak bioluminescence in each of the tissues sampled in the TG and WT mice at 6 and 12 months of age. Circular variances, which reflect the variation in the angles about the mean phase angle, were computed for each individual mouse (Fig. 4C). Only mice with detectable circadian oscillations in every sampled tissue were included. We excluded the liver from this particular analysis because n = 9 were arrhythmic. Mann-Whitney tests indicated no difference in circular variance between PER2::LUC and APP/PS1xPER2::LUC at 6 months (U = 59, $p = 0.320$) or 12 months (U = 22, $p = 0.805$) of age. Representative PER2::LUC bioluminescence in the SCN and spleen are shown in Supplementary Figure S8.

3.10. APP/PS1 mice do not exhibit altered food-anticipatory activity

The SCN controls the timing of circadian oscillators in peripheral tissues in part by generating a daily rhythm of food intake. In nocturnal rodents, most eating occurs at night, and metabolic rhythms and organ functions are synchronized accordingly. If food is made available only during the light period, the normal fasting phase, most peripheral oscillators dissociate from the SCN and shift to realign with daytime food intake. An SCN-independent behavioral rhythm of food-anticipatory activity also emerges (Mistlberger, 2009). To determine whether the APP/PSI transgenes alter the response of the circadian system to a shift of mealtime, mice at 9.5 months and 19 months of age were gradually introduced to daytime feeding by alternating bouts of 18 hours of food deprivation starting at lights-off with 30 hour bouts of food access starting in the middle of the 12 hour light period (6 hours after lights-on). After 4 cycles on this regimen, food availability was limited to hours 6–12 of the light period. This was gradually reduced to 4 hours (hours 6–10 of the light period). Circadian rhythms of food-anticipatory activity were quantified by calculating the fraction of total daily activity, recorded by infrared motion sensors that occurred in the 4 hours immediately preceding the meal (Fig. 5). Independent *t*-tests revealed no statistically significant differences between genotype in

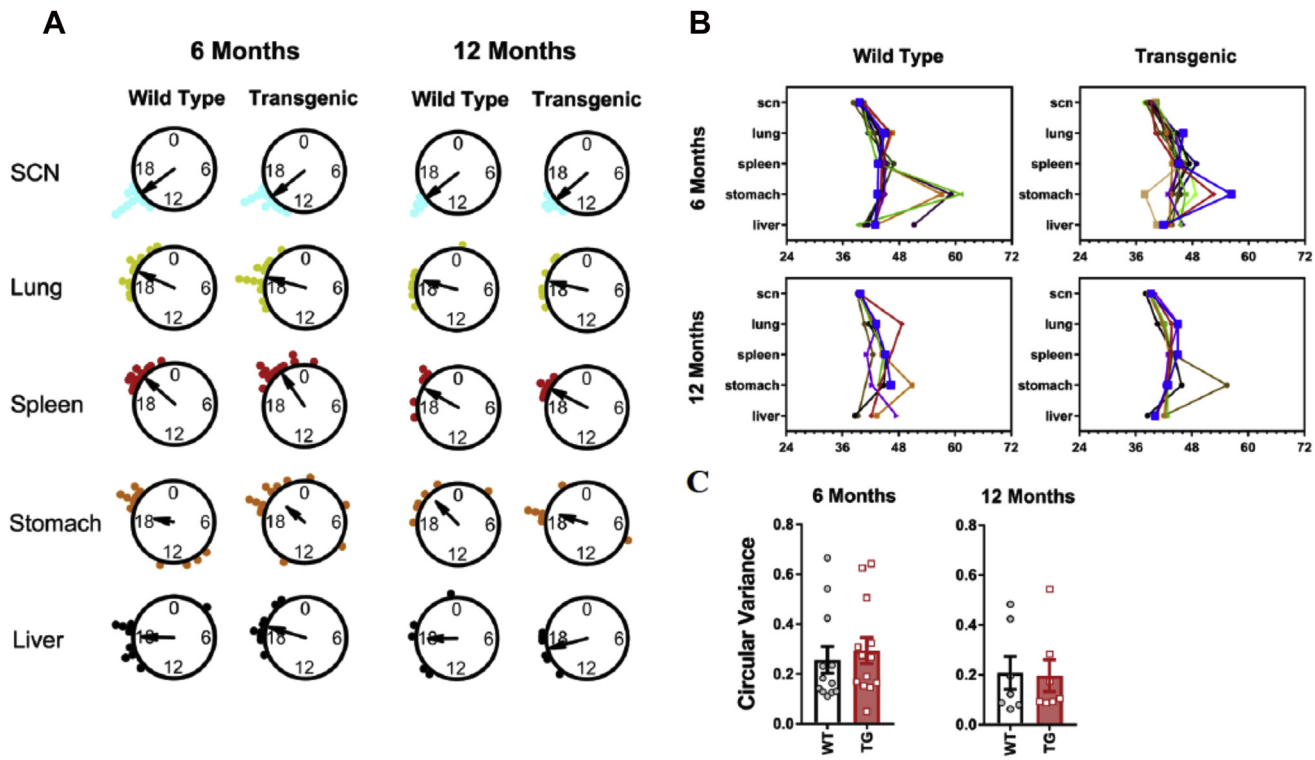

Fig. 4. PER2::LUC bioluminescence in various tissues of APP/PS1xPER2::LUC mice. (A) Circular diagrams of the first peak of PER2::LUC bioluminescence after 24 hours in culture. Each dot represents peak bioluminescence for 1 mouse relative to time of lights-on in the colony room (ZT0). Arrow direction corresponds to mean phase angle. Arrow lengths are inversely proportional to the circular variance of the data. (B) Phase diagrams of peak bioluminescence for mice shown in A. Each color corresponds to an individual mouse. The x-axis is hours since lights-on (ZT0) on day of sacrifice. (C) Circular variances of individual mice. TG data are shown in red and WT data are shown in black. Data are expressed as the mean ± SEM. (For interpretation of the references to color in this figure legend, the reader is referred to the Web version of this article.)

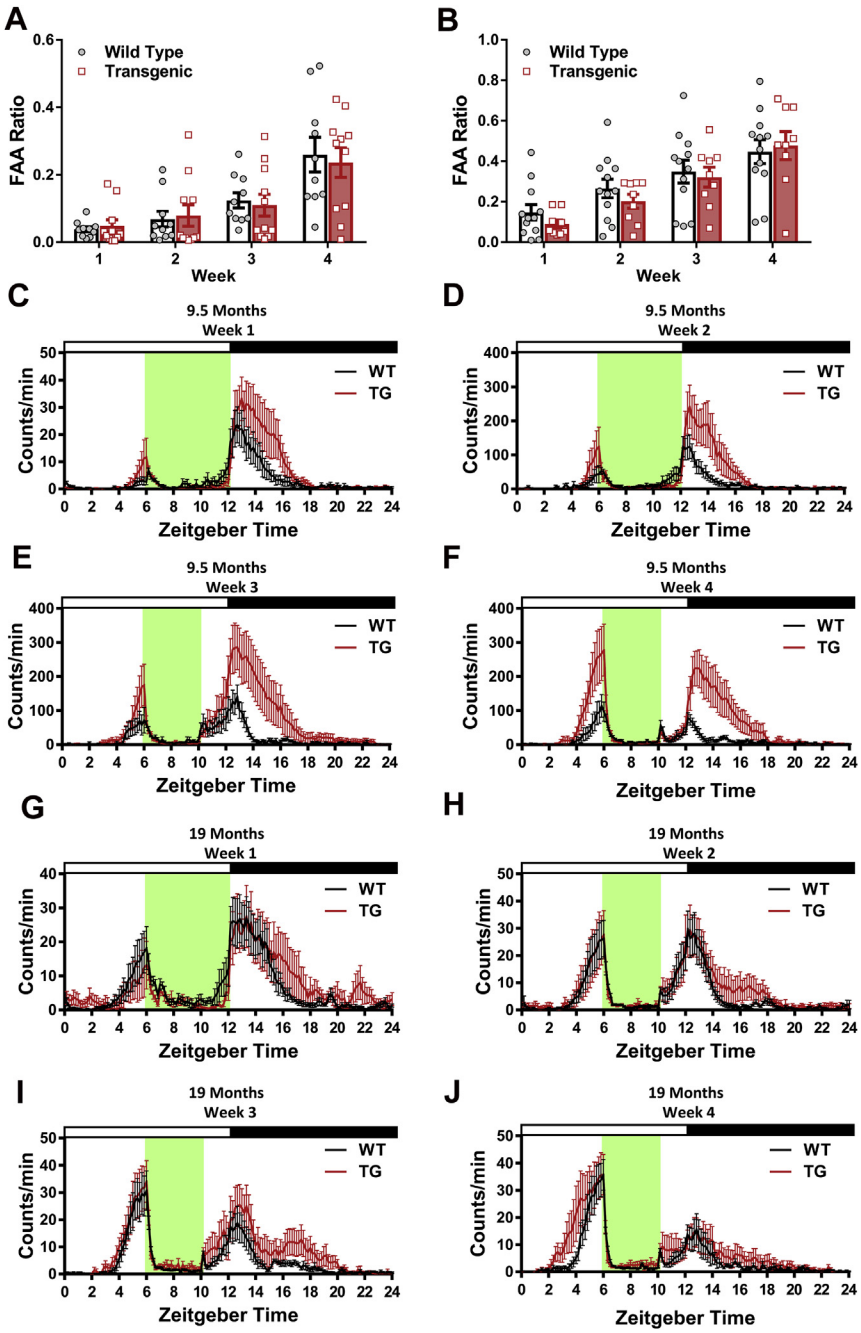

Fig. 5. Food-anticipatory activity (FAA) trajectory at 9.5 months age (A) and 19 months of age (B), following 1–4 weeks of a restricted feeding schedule. Food-anticipatory activity at 9.5 months (C–F) and 19 months of age (G–J), following 1–4 weeks of a restricted feeding schedule. The feeding windows are represented by the green shading. TG data are shown in red and the WT data are shown in black. Data are expressed as the mean ± SEM. (For interpretation of the references to color in this figure legend, the reader is referred to the Web version of this article.)

the food anticipation ratio during weeks 1–4 of restricted feeding at either age (Fig. 5A and B, all $p > 0.05$). Fig. 5C–J shows cage activity across the 24 hour day, recorded by infrared motion sensors. Independent *t*-tests revealed no statistically significant differences between genotype during weeks 1–4 of restricted feeding at either age (all $p > 0.05$).

3.11. The EEG power spectra shifts to higher frequencies in APP/PS1 mice at 12 months of age

To evaluate whether sleep was affected in the APP/PS1 mouse model, mice were fitted with cranial implants of EEG/EMG electrodes. The final 24 hours of EEG recordings were examined to assess whether there were state-dependent EEG power spectra shifts associated with genotype. Fig. 6 shows the normalized power spectra for wake (Fig. 6A), NREM (Fig. 6B), and REM (Fig. 6C) states. Two-way ANOVAs revealed statistically significant interactions between genotype and frequency on power density for wake ($p = 0.0007$, F [50, 510] = 1.83) and NREM ($p < 0.0001$, F [50, 510] = 9.254) but not for REM ($p > 0.05$).

To examine which frequency bands were specifically affected, the normalized power spectra from the 24 hour recordings were binned into delta (0.1–4.0 Hz), theta (4.1–8.0 Hz), alpha (8.1–13 Hz), beta (13.1–30 Hz), and gamma (30.1–50 Hz)

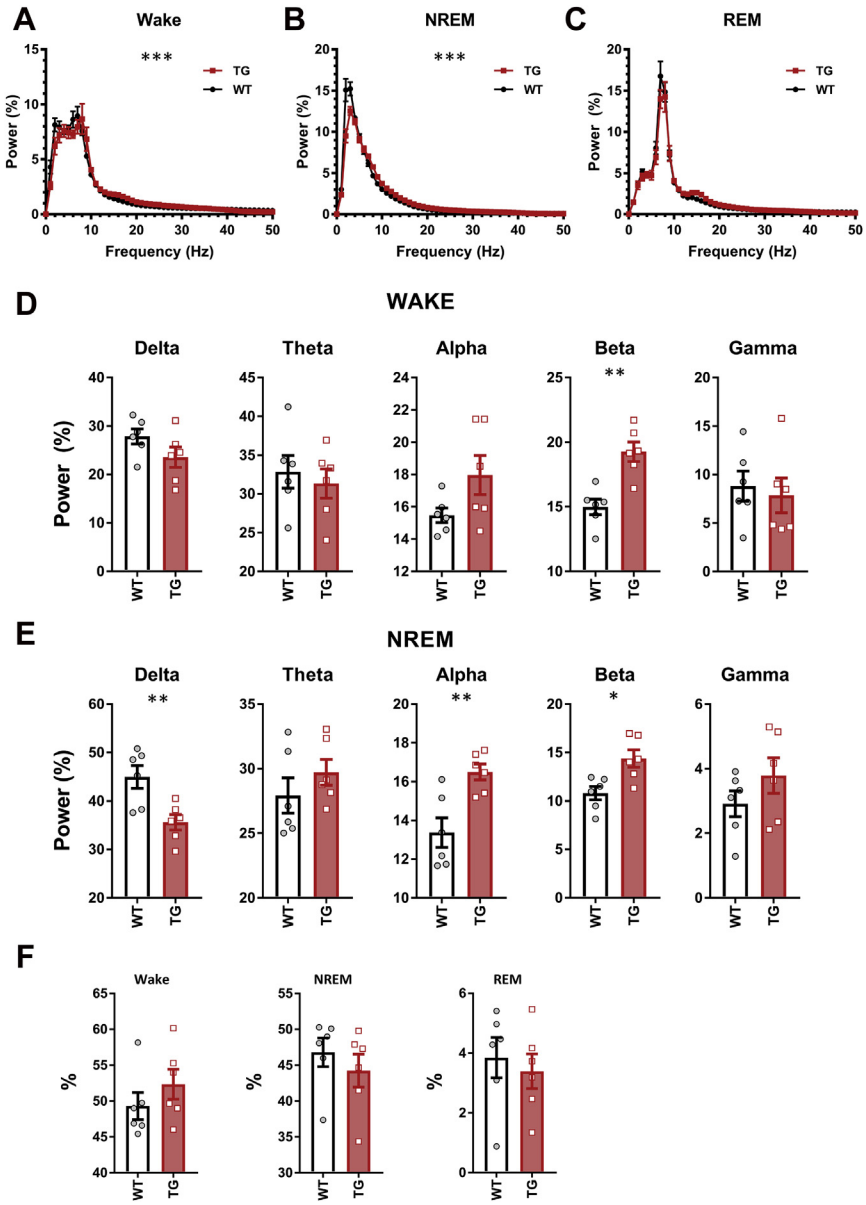

Fig. 6. EEG normalized power spectra of the APP/PS1 mouse model and WT mice at 12 months of age for wake (A), NREM (B), and REM (C) states. Data expressed as percent of total power across frequencies 0.1–50 Hz. ** $p < 0.01$, *** $p < 0.001$ interaction, 2-way ANOVA. Power band comparison for delta (0.1–4 Hz), theta (4–8 Hz), alpha (8–13 Hz), beta (13.1–30 Hz), and gamma (30.1–50 Hz) frequency bands during wake (D) and NREM (E) states. TG data are shown in red and the WT data are shown in black. * $p < 0.05$, ** $p < 0.01$, independent *t*-test. No differences between genotypes in the percentage of time spent awake, in NREM, or in REM stages over a 24-hour period (F). * $p < 0.05$, ** $p < 0.01$, independent *t*-test. TG data are shown in red and the WT data are shown in black. All data are expressed as mean ± SEM. n = 6/group. (For interpretation of the references to color in this figure legend, the reader is referred to the Web version of this article.)

frequency bands. Only the power spectra that showed statistically significant interactions between genotype and frequency were evaluated at specific frequency bands. Fig. 6 shows the power band comparisons for wake (Fig. 6D) and NREM (Fig. 6E). During wake, independent *t*-tests showed a significant increase in beta power in TG compared to WT ($p = 0.0013$, $t = 4.425$, df = 10) but not in the other bands ($p > 0.05$). During the NREM state, independent *t*-tests showed significant differences in the delta (decreased in TG; $p = 0.0080$, $t = 3.299$, df = 10), alpha (increased in TG; $p = 0.0050$, $t = 3.583$, df = 10), and beta (increased in TG; $p = 0.0103$, $t = 3.151$, df = 10) bands but not in the theta or gamma bands ($p > 0.05$).

To examine whether the state-dependent EEG power spectra shifts were also observed in the raw, non-normalized power spectra, the power spectra for the TG and WT were compared for wake, NREM, and REM states. Supplementary Fig. S9 shows the raw power spectra. Two-way ANOVAs revealed a statistically significant interaction between genotype and frequency on raw power for the NREM state ($p < 0.0001$, $F(50, 510) = 2.566$) but not for wake or REM states ($p > 0.05$).

To evaluate whether the reduced slow-wave activity was due to changes in total time spent asleep, we assessed the amount of time spent in wake, NREM, and REM states during the final 24 hours of the EEG recordings (Fig. 6F). TG and WT were compared using independent *t*-tests. There were no statistically significant differences between TG and WT for the amount of time spent in wake, NREM, or REM stages ($p > 0.05$). The reduced slow-wave activity was not due to changes in total sleep time.

4. Discussion

There is growing evidence that changes in circadian rhythms and sleep occur early in AD, and the underlying mechanisms leading to these changes may offer insight into the disease pathophysiology and the development of novel therapeutic interventions. To model these disease mechanisms, we pursued a detailed analysis of an AD mouse model previously shown to have a sleep and circadian phenotype (Roh et al., 2012).

The mice were examined from 5 to 22 months of age using a mix of both longitudinal and cross-sectional experimental designs. The TG developed Aβ plaques by 7 months of age and exhibited a small and persistent delay in onset of daily nocturnal physical activity by 5 months of age. The delayed phase of entrainment to LD is reminiscent of findings from human patients with AD who exhibit a delayed phase in daily rhythms of activity and core body temperature (Harper et al., 2001, 2004, 2005). To investigate the mechanism underlying the delayed angle of entrainment in the APP/PS1 mouse model, we assessed a comprehensive set of circadian measures including differences in endogenous period length (τ), total daily activity, and light sensitivity through responses to a light pulse or phase advance in the LD schedule. None of these measures revealed differences between TG and WT mice. To assess circadian dynamics outside the SCN, we evaluated synchrony of select oscillators in the APP/PS1xPER2:LUC mouse model but found no differences between TG and WT. We also found no differences in rate of food entrainment between TG and WT mice. Taken together, it is unclear what is causing the delayed phase of entrainment in this mouse model. Because there is no evidence for any change in clock input or endogenous period (τ), it is possible that there are changes in clock output, such as a change in coupling between SCN and secondary oscillators downstream, beyond those examined here, that regulate more directly the rest-activity cycle.

In addition to evaluating circadian rhythmicity, we also evaluated sleep in the APP/PS1 mouse model. There were no differences between TG and WT in time spent in wake, NREM, or REM states; however, the TG exhibited a shift in EEG power spectra to higher frequencies, with a significant reduction in the slow-wave delta power during NREM sleep compared to WT. Interestingly, these findings are consistent with our previous work using the congenic APPswe/PS1dE9 mouse model, which also demonstrates reduced delta power in NREM sleep (Kent et al., 2018). Future studies will be required to fully elucidate the relationship with these state-dependent quantitative EEG findings in rodents and reports of reduced slow-wave sleep observed in human patients with AD (Bliwise et al., 1989; Hot et al., 2011; Loewenstein et al., 1982; Prinz et al., 1982; Vitiello et al., 1990). Reduced delta power during NREM may represent a sensitive and potentially modifiable measure of disrupted sleep in AD.

Previous research examining circadian rhythms and sleep in this model has been limited. Otalora et al. (2012) reported higher levels of activity in the $APP_{SWE}/PS1_{dE9}$, compared to the WT (Bano Otalora et al., 2012). The TG mice did not show any differences compared to WT in free-running period or in time to re-entrain after a 6 hour phase advance in the LD cycle (Bano Otalora et al., 2012). These findings are similar to what we show here; however, in their study, there was no difference in activity onset between the TG and WT, which is in contrast to the delay in activity onset observed in our cohorts. Disturbances in sleep regulation in $APP_{SWE}/PS1_{dE9}$ mice have been reported in another study in mice aged 6–9 months (Roh et al., 2012) in which TG mice exhibited marked disruption of the sleep-wake cycle, characterized as increased wakefulness and reductions in both REM and non-REM sleep (Roh et al., 2012). This study only assessed daily activity for 2 days and also did not evaluate circadian parameters. In our study, the EEG recordings did show a trend toward more wakefulness but was not statistically significant. It is possible that the amount of wakefulness or the time spent in specific sleep stages is affected at a later age not tested here.

Jyoti et al. (2010) examined a similar model, the $APP_{SWE}/PS1_{A246E}$, and saw no changes in circadian behavior but only evaluated daily rhythms in activity for 5 days in LD, without any other probes to evaluate circadian parameters (Jyoti et al., 2010). The most striking effect from their study was that at 5 months of age, the APP/PS1 mice exhibited higher activity levels than WT controls, and at 5 months and 20 months of age, they exhibited more wakefulness and less NREM sleep (Jyoti et al., 2010). A phase delay in activity onset was reported in another APP/PS1 model ($APP_{NLH}/PS1_{P264L}$) (Duncan et al., 2012). In that study, the transgenic mice exhibited phase delays of ~2 hours in the onset of wakefulness bouts measured by piezoelectric recordings (Duncan et al., 2012). Interestingly, the effect of genotype on activity onset was not detected in the activity data collected via running wheels (Duncan et al., 2012), highlighting how experimental design can greatly affect assay sensitivity.

In addition to phenotyping the APP/PS1 mouse model, we also created a novel mouse model by crossing APP/PS1 mice with the PER2::LUC model, enabling us to evaluate circadian synchrony of PER2 expression in several tissues. Uncoupling or misalignment among peripheral oscillators would cause similar behavioral symptoms to a dampening of SCN processes but would require different interventions to correct. Previous work suggests that AD pathology may affect peripheral synchrony (Cermakian et al., 2011; Chauhan et al., 2017; Chen et al., 2014; Kent, 2014). For example, a *drosophila* model that expresses human Aβ was found to exhibit progressive behavioral arrhythmia, despite the normal oscillation of the central molecular clock, suggesting a failure of the central clock to entrain downstream peripheral oscillators (Chen et al., 2014). Furthermore, a human postmortem study looked at clock gene expression in various brain structures and found that individuals with AD exhibited marked phase shifts in brain structures outside the SCN, suggesting reduced synchronization (Cermakian et al., 2011). Aβ has also been found to have effects on peripheral circadian clocks in human fibroblasts (Wilkaniec et al., 2016). Taken together these results indicate that some sources of circadian disruption in AD may lie outside the central clock; however, APP/PS1xPER2::LUC mice showed no differences in synchrony between the 4 extra-SCN oscillators examined here at 6 months and 12 months of age.

Despite the lack of evidence for internal desynchrony in APP/PSI mice, our screen was limited to 4 peripheral tissues, and it remains possible that coupling between the SCN and local oscillators elsewhere in the brain and body is disrupted. Peripheral clocks not examined here could be important, such as timing in the hippocampus and other brain regions. Local circadian oscillators are present in numerous brain regions, but oscillations in these tissues are less robust in vitro and more likely to be reset by the explant procedure, making assessment of internal synchrony more difficult. Furthermore, given the progressive nature of the APP/PS1 mouse model, it is possible that internal synchrony becomes altered at a later age not tested here.

An important limitation of the present study is that it was not powered to investigate sex differences. As noted in Figure S3, at 3–4 months of age, we observed a delay of activity onset in female, but not in male TG mice, suggesting that phenotypes may show up earlier and be more pronounced in females. The EEG analysis was only assessed in females, so future studies should assess whether the same shift in power spectra is observed in male APP/PS1 mice. On a similar note, at 9.5 months of age, the TG appear to have a drastic increase in activity when food is presented and when lights

go off compared to WT mice (Fig. 5C–F). This is something that we cannot explain but is driven by 3 male mice (see Supplementary Fig. S1G-H for actograms). This mouse model has been reported to exhibit higher levels of activity (Bano Otalora et al., 2012), although we did not see higher activity in the TG in our cohorts when they were under *ad lib* feeding conditions. Because of the small sample sizes, we are not able to draw conclusions about sex differences, but this is something that could be explored in future studies.

Finally, it is important to note that the APP/PS1 mouse model only approximates the progressive Aβ accumulation seen in AD, and not the other pathological hallmarks, including neurofibrillary tangles and neurodegeneration. Transgenic mouse models are thought to best model the earliest stages of AD before widespread synaptic loss. Insofar as the sleep and circadian disturbances associated with AD occur later in the disease course, or involve mechanisms unique to human pathophysiology, these mechanisms may be difficult to elucidate using transgenic mouse models.

5. Conclusions

Overall, the APP/PS1 mouse model exhibits a subtle circadian phenotype. The slight but persistent delay in phase of entrainment to LD is similar to the delay in activity and temperature rhythms identified in patients with AD, but as these changes do not worsen with age in APP/PS1 mice, progressive Aβ accumulation is unlikely to drive this phenotype. There were also no other profound effects of the transgenes on the numerous circadian parameters explored. Although the mechanisms underlying impairments in circadian rhythmicity in AD remain of significant interest, the lack of a robust and progressive central or peripheral circadian phenotype across ages suggest that the current APP/PS1 mouse model may not be the optimal preclinical model to further evaluate these important mechanisms. Emerging data suggest that changes in slow-wave sleep may be directly linked to Aβ pathophysiology, and our findings indicate that quantitative EEG represents a sensitive measure of sleep quality that can be consistently modeled in APP/PS1 mice. Future studies are required to assess the value of quantitative EEG across the human AD spectrum, preferably through ambulatory EEG monitoring.

Disclosure

The authors declare that they have no competing interests.

Acknowledgements

The authors are grateful to Sylvie Couture-Nowak, Sarah Power, and Andrea Smit for their assistance with the experiments.

The authors gratefully acknowledge grant funding from NSERC, Canada (REM, grant #04200), MSFHR, Canada (BAK, HBN), Killam Trusts, Canada (BAK), CIHR Banting, Canada (BAK), and NSERC doctoral fellowship (MM).

Ethics approval and consent to participate: All procedures involving experimental animals were approved by the Canadian Council of Animal Care, the University of British Columbia Committee on Animal Care, and the Simon Fraser University Animal Care Committee (permit 1106p-09).

Availability of data and material: The data sets used and/or analyzed during the present study are available from the corresponding author on request.

Authors' contributions: BAK, MM, REM, and HBN designed the experiments. BAK, MM, EGM, and KY conducted the experiments and analyses. BAK, MM, REM, and HBN wrote the article. HHF contributed to reviewing and interpreting the data and article. All authors read and approved the final article.

Appendix A. Supplementary data

Supplementary data associated with this article can be found, in the online version, at https://doi.org/10.1016/j.neurobiolaging.2019.01.010.

References

Bano Otalora, B., Popovic, N., Gambini, J., Popovic, M., Vina, J., Bonet-Costa, V., Reiter, R.J., Camello, P.J., Rol, M.A., Madrid, J.A., 2012. Circadian system functionality, hippocampal oxidative stress, and spatial memory in the APPswe/PS1dE9 transgenic model of Alzheimer disease: effects of melatonin or ramelteon. Chronobiol. Int. 29, 822–834.

Bianchetti, A., Scuratti, A., Zanetti, O., Binetti, G., Frisoni, G.B., Magni, E., Trabucchi, M., 1995. Predictors of mortality and institutionalization in Alzheimer disease patients 1 year after discharge from an Alzheimer dementia unit. Dementia 6, 108–112.

Bliwise, D.L., Tinklenberg, J., Yesavage, J.A., Davies, H., Pursley, A.M., Petta, D.E., Dement, W.C., 1989. REM latency in Alzheimer's disease. Biol. Psychiatry. 25, 320–328.

Cedernaes, J., Osorio, R.S., Varga, A.W., Kam, K., Schioth, H.B., Benedict, C., 2017. Candidate mechanisms underlying the association between sleep-wake disruptions and Alzheimer's disease. Sleep Med. Rev. 31, 102–111.

Cermakian, N., Lamont, E.W., Boudreau, P., Boivin, D.B., 2011. Circadian clock gene expression in brain regions of Alzheimer 's disease patients and control subjects. J. Biol. Rhythms. 26, 160–170.

Chauhan, R., Chen, K.F., Kent, B.A., Crowther, D.C., 2017. Central and peripheral circadian clocks and their role in Alzheimer's disease. Dis. Model. Mech. 10, 1187–1199.

Chen, K.F., Possidente, B., Lomas, D.A., Crowther, D.C., 2014. The central molecular clock is robust in the face of behavioural arrhythmia in a Drosophila model of Alzheimer's disease. Dis. Model. Mech. 7, 445–458.

Dijk, D.J., Czeisler, C.A., 1995. Contribution of the circadian pacemaker and the sleep homeostat to sleep propensity, sleep structure, electroencephalographic slow waves, and sleep spindle activity in humans. J. Neurosci. 15, 3526–3538.

Duncan, M.J., Smith, J.T., Franklin, K.M., Beckett, T.L., Murphy, M.P., St Clair, D.K., Donohue, K.D., Striz, M., O'Hara, B.F., 2012. Effects of aging and genotype on circadian rhythms, sleep, and clock gene expression in APPxPS1 knock-in mice, a model for Alzheimer's disease. Exp. Neurol. 236, 249–258.

Gordon, B.A., Blazey, T.M., Su, Y., Hari-Raj, A., Dincer, A., Flores, S., Christensen, J., McDade, E., Wang, G., Xiong, C., Cairns, N.J., Hassenstab, J., Marcus, D.S., Fagan, A.M., Jack Jr., C.R., Hornbeck, R.C., Paumier, K.L., Ances, B.M., Berman, S.B., Brickman, A.M., Cash, D.M., Chhatwal, J.P., Correia, S., Forster, S., Fox, N.C., Graff-Radford, N.R., la Fougere, C., Levin, J., Masters, C.L., Rossor, M.N., Salloway, S., Saykin, A.J., Schofield, P.R., Thompson, P.M., Weiner, M.M., Holtzman, D.M., Raichle, M.E., Morris, J.C., Bateman, R.J., Benzinger, T.L.S., 2018. Spatial patterns of neuroimaging biomarker change in individuals from families with autosomal dominant Alzheimer's disease: a longitudinal study. Lancet Neurol. 17, 241–250.

Guarnieri, B., Adorni, F., Musicco, M., Appollonio, I., Bonanni, E., Caffarra, P., Caltagirone, C., Cerroni, G., Concari, L., Cosentino, F.I., Ferrara, S., Fermi, S., Ferri, R., Gelosa, G., Lombardi, G., Mazzei, D., Mearelli, S., Morrone, E., Murri, L., Nobili, F.M., Passero, S., Perri, R., Rocchi, R., Sucapane, P., Tognoni, G., Zabberoni, S., Sorbi, S., 2012. Prevalence of sleep disturbances in mild cognitive impairment and dementing disorders: a multicenter Italian clinical cross-sectional study on 431 patients. Dement. Geriatr. Cogn. Disord. 33, 50–58.

Harper, D.G., Stopa, E.G., McKee, A.C., Satlin, A., Fish, D., Volicer, L., 2004. Dementia severity and Lewy bodies affect circadian rhythms in Alzheimer disease. Neurobiol. Aging. 25, 771–781.

Harper, D.G., Stopa, E.G., McKee, A.C., Satlin, A., Harlan, P.C., Goldstein, R., Volicer, L., 2001. Differential circadian rhythm disturbances in men with Alzheimer disease and frontotemporal degeneration. Arch. Gen. Psychiatry. 58, 353–360.

Harper, D.G., Volicer, L., Stopa, E.G., McKee, A.C., Nitta, M., Satlin, A., 2005. Disturbance of endogenous circadian rhythm in aging and Alzheimer disease. Am. J. Geriatr. Psychiatry. 13, 359–368.

Hot, P., Rauchs, G., Bertran, F., Denise, P., Desgranges, B., Clochon, P., Eustache, F., 2011. Changes in sleep theta rhythm are related to episodic memory impairment in early Alzheimer's disease. Biol. Psychol. 87, 334–339.

Jankowsky, J.L., Fadale, D.J., Anderson, J., Xu, G.M., Gonzales, V., Jenkins, N.A., Copeland, N.G., Lee, M.K., Younkin, L.H., Wagner, S.L., Younkin, S.G., Borchelt, D.R., 2004. Mutant presenilins specifically elevate the levels of the 42 residue β-amyloid peptide in vivo: evidence for augmentation of a 42-specific γ secretase. Hum. Mol. Genet. 13, 159–170.

Ju, Y.E., Lucey, B.P., Holtzman, D.M., 2014. Sleep and Alzheimer disease pathology–a bidirectional relationship. Nat. Rev. Neurol. 10, 115–119.

Ju, Y.S., Ooms, S.J., Sutphen, C., Macauley, S.L., Zangrilli, M.A., Jerome, G., Fagan, A.M., Mignot, E., Zempel, J.M., Claassen, J., Holtzman, D.M., 2017. Slow wave sleep

disruption increases cerebrospinal fluid amyloid-beta levels. Brain 140, 2104–2111.
Jyoti, A., Plano, A., Riedel, G., Platt, B., 2010. EEG, activity, and sleep architecture in a transgenic AbetaPPswe/PSEN1A246E Alzheimer's disease mouse. J. Alzheimers. Dis. 22, 873–887.
Kent, B.A., 2014. Synchronizing an aging brain: can entraining circadian clocks by food slow Alzheimer's disease? Front. Aging. Neurosci. 6, 234.
Kent, B.A., Strittmatter, S.M., Nygaard, H.B., 2018. Sleep and EEG power spectral analysis in three transgenic mouse models of AD: APP/PS1, 3xTgAD, and Tg2576. J. Alzhiemers. Dis. 64, 1325–1336.
Knight, E.M., Brown, T.M., Gumusgoz, S., Smith, J.C., Waters, E.J., Allan, S.M., Lawrence, C.B., 2013. Age-related changes in core body temperature and activity in triple-transgenic Alzheimer's disease (3xTgAD) mice. Dis. Model. Mech. 6, 160–170.
La Morgia, C., Ross-Cisneros, F.N., Koronyo, Y., Hannibal, J., Gallassi, R., Cantalupo, G., Sambati, L., Pan, B.X., Tozer, K.R., Barboni, P., Provini, F., Avanzini, P., Carbonelli, M., Pelosi, A., Chui, H., Liguori, R., Baruzzi, A., Koronyo-Hamaoui, M., Sadun, A.A., Carelli, V., 2016. Melanopsin retinal ganglion cell loss in Alzheimer disease. Ann. Neurol. 79, 90–109.
La Morgia, C., Ross-Cisneros, F.N., Sadun, A.A., Carelli, V., 2017. Retinal ganglion cells and circadian rhythms in Alzheimer's disease, Parkinson's disease, and beyond. Front. Neurol. 8, 162.
Loewenstein, R.J., Weingartner, H., Gillin, J.C., Kaye, W., Ebert, M., Mendelson, W.B., 1982. Disturbances of sleep and cognitive functioning in patients with dementia. Neurobiol. Aging. 3, 371–377.
Lucey, B.P., Hicks, T.J., McLeland, J.S., Toedebusch, C.D., Boyd, J., Elbert, D.L., Patterson, B.W., Baty, J., Morris, J.C., Ovod, V., Mawuenyega, K.G., 2018. Effect of sleep on overnight CSF amyloid-β kinetics. Ann. Neurol. 83, 197–204.
Mander, B.A., Winer, J.R., Jagust, W.J., Walker, M.P., 2016. Sleep: a novel mechanistic pathway, biomarker, and treatment target in the pathology of Alzheimer's disease? Trends. Neurosci. 39, 552–566.
Mistlberger, R.E., 2009. Food-anticipatory circadian rhythms: concepts and methods. Eur. J. Neurosci. 30, 1718–1729.
Musiek, E.S., Bhimasani, M., Zangrilli, M.A., Morris, J.C., Holtzman, D.M., Ju, Y.S., 2018. Circadian rest-activity pattern changes in aging and preclinical Alzheimer disease. JAMA Neurol. 75, 582–590.
Nygaard, H.B., 2013. Current and emerging therapies for Alzheimer's disease. Clin. Ther. 35, 1480–1489.
Perez, S.E., Lumayag, S., Kovacs, B., Mufson, E.J., Xu, S., 2009. Beta-amyloid deposition and functional impairment in the retina of the APPswe/PS1DeltaE9 transgenic mouse model of Alzheimer's disease. Invest. Ophthalmol. Vis. Sci. 50, 793–800.
Pittendrigh, C.S., Daan, S., 1976. A functional analysis of circadian pacemakers in nocturnal rodents - IV. Entrainment: pacemaker as clock. J. Comp. Physiol. 106, 291–331.
Prinz, P.N., Peskind, E.R., Vitalino, P.P., Raskind, M.A., Eisdorfer, C., Zemcuznikov, H.N., Gerber, C.J., 1982. Changes in the sleep and waking EEGs of nondemented and demented elderly subjects. J. Am. Geriatr. Soc. 30, 86–92.
Reppert, S.M., Weaver, D.R., 2002. Coordination of circadian timing in mammals. Nature 418, 935–941.
Roh, J.H., Huang, Y., Bero, A.W., Kasten, T., Stewart, F.R., Bateman, R.J., Holtzman, D.M., 2012. Disruption of the sleep-wake cycle and diurnal fluctuation of beta-amyloid in mice with Alzheimer's disease pathology. Sci. Transl. Med. 4, 150ra122.
Satlin, A., Volicer, L., Stopa, E.G., Harper, D., 1995. Circadian locomotor activity and core-body temperature rhythms in Alzheimer's disease. Neurobiol. Aging. 16, 765–771.
Sethi, M., Joshi, S.S., Webb, R.L., Beckett, T.L., Donohue, K.D., Murphy, M.P., O'Hara, B.F., Duncan, M.J., 2015. Increased fragmentation of sleep-wake cycles in the 5XFAD mouse model of Alzheimer's disease. Neuroscience 290, 80–89.
Sterniczuk, R., Dyck, R.H., Laferla, F.M., Antle, M.C., 2010. Characterization of the 3xTg-AD mouse model of Alzheimer's disease: part 1. Circadian changes. Brain. Res. 1348, 139–148.
Tranah, G.J., Blackwell, T., Stone, K.L., Ancoli-Israel, S., Paudel, M.L., Ensrud, K.E., Cauley, J.A., Redline, S., Hillier, T.A., Cummings, S.R., Yaffe, K., Group, S.O.F.R., 2011. Circadian activity rhythms and risk of incident dementia and mild cognitive impairment in older women. Ann. Neurol. 70, 722–732.
Vitiello, M.V., Prinz, P.N., Williams, D.E., Frommlet, M.S., Ries, R.K., 1990. Sleep disturbances in patients with mild-stage Alzheimer's disease. J. Gerontol. 45, M131–M138.
Vloeberghs, E., Van Dam, D., Engelborghs, S., Nagels, G., Staufenbiel, M., De Deyn, P.P., 2004. Altered circadian locomotor activity in APP23 mice: a model for BPSD disturbances. Eur. J. Neurosci. 20, 2757–2766.
Volicer, L., Harper, D.G., Manning, B.C., Goldstein, R., Satlin, A., 2001. Sundowning and circadian rhythms in Alzheimer's disease. Am. J. Psychiatry. 158, 704–711.
Watanabe, T., Kajimura, N., Kato, M., Sekimoto, M., Nakajima, T., Hori, T., Takahashi, K., 2003. Sleep and circadian rhythm disturbances in patients with delayed sleep phase syndrome. Sleep 26, 657–661.
Webb, I.C., Antle, M.C., Mistlberger, R.E., 2014. Regulation of circadian rhythms in mammals by behavioral arousal. Behav. Neurosci. 128, 304–325.
Wilkaniec, A., Schmitt, K., Grimm, A., Strosznajder, J.B., Eckert, A., 2016. Alzheimer's amyloid-beta peptide disturbs P2X7 receptor-mediated circadian oscillations of intracellular calcium. Folia. Neuropathol. 54, 360–368.
Witting, W., Kwa, I.H., Eikelenboom, P., Mirmiran, M., Swaab, D.F., 1990. Alterations in the circadian rest-activity rhythm in aging and Alzheimer's disease. Biol. Psychiatry. 27, 563–572.
Wu, Y.H., Fischer, D.F., Kalsbeek, A., Garidou-Boof, M.L., van der Vliet, J., van Heijningen, C., Liu, R.Y., Zhou, J.N., Swaab, D.F., 2006. Pineal clock gene oscillation is disturbed in Alzheimer's disease, due to functional disconnection from the "master clock". FASEB. J. 20, 1874–1876.
Xie, L., Kang, H., Xu, Q., Chen, M.J., Liao, Y., Thiyagarajan, M., O'Donnell, J., Christensen, D.J., Nicholson, C., Iliff, J.J., Takano, T., Deane, R., Nedergaard, M., 2013. Sleep drives metabolite clearance from the adult brain. Science 342, 373–377.
Yaffe, K., Nettiksimmons, J., Yesavage, J., Byers, A., 2015. Sleep quality and risk of dementia among older male veterans. Am. J. Geriatr. Psychiatry. 23, 651–654.
Yamazaki, S., Takahashi, J.S., 2005. Real-time luminescence reporting of circadian gene expression in mammals. Methods. Enzymol. 393, 288–301.
Yoo, S.H., Yamazaki, S., Lowrey, P.L., Shimomura, K., Ko, C.H., Buhr, E.D., Menaker, M., Takahashi, J.S., 2004. PERIOD2::LUCIFERASE real-time reporting of circadian dynamics reveals persistent circadian oscillations in mouse peripheral tissues. Proc. Natl. Acad. Sci. U. S. A. 101, 5339–5346.